PCP
PLANT & CELL PHYSIOLOGY

Cell Wall Polysaccharides are Mislocalized to the Vacuole in *echidna* Mutants

Heather E. McFarlane[1,3], Yoichiro Watanabe[1,3], Delphine Gendre[2], Kimberley Carruthers[1], Gabriel Levesque-Tremblay[1], George W. Haughn[1], Rishikesh P. Bhalerao[2] and Lacey Samuels[1,*]

[1]Department of Botany, University of British Columbia, Vancouver, BC, Canada V6T 1Z4
[2]Umeå Plant Science Centre, Department of Forest Genetics and Plant Physiology, Swedish University of Agricultural Sciences, S-901 83 Umeå, Sweden
[3]These authors contributed equally to this work.
*Corresponding author: E-mail, lsamuels@mail.ubc.ca; Fax +1-604-822-6089.
(Received July 8, 2013; Accepted September 9, 2013)

During cell wall biosynthesis, the Golgi apparatus is the platform for cell wall matrix biosynthesis and the site of packaging, of both matrix polysaccharides and proteins, into secretory vesicles with the correct targeting information. The objective of this study was to dissect the post-Golgi trafficking of cell wall polysaccharides using *echidna* as a vesicle traffic mutant of *Arabidopsis thaliana* and the pectin-secreting cells of the seed coat as a model system. *ECHIDNA* encodes a *trans*-Golgi network (TGN)-localized protein, which was previously shown to be required for proper structure and function of the secretory pathway. In *echidna* mutants, some cell wall matrix polysaccharides accumulate inside cells, rather than being secreted to the apoplast. In this study, live cell imaging of fluorescent protein markers as well as transmission electron microscopy (TEM)/immunoTEM of cryofixed seed coat cells were used to examine the consequences of TGN disorganization in *echidna* mutants under conditions of high polysaccharide production and secretion. While in wild-type seed coat cells, pectin is secreted to the apical surface, in *echidna*, polysaccharides accumulate in post-Golgi vesicles, the central lytic vacuole and endoplasmic reticulum-derived bodies. In contrast, proteins were partially mistargeted to internal multilamellar membranes in *echidna*. These results suggest that while secretion of both cell wall polysaccharides and proteins at the TGN requires ECHIDNA, different vesicle trafficking components may mediate downstream events in their secretion from the TGN.

Keywords: Arabidopsis • Polysaccharide • Secretion • Seed coat • *Trans*-Golgi network.

Abbreviations: CFP, cyan fluorescent protein; ECH, ECHIDNA; ER, endoplasmic reticulum; GFP, green fluorescent protein; PIP2, plasma membrane intrinsic protein 2; RNAi, RNA interference; RT–PCR, reverse transcription–PCR; SEM, scanning electron microscopy; SNARE, soluble NSF (*N*-ethylmaleimide-sensitive factor) attachment protein receptor; TBS, Tris-buffered saline; TEM, transmission electron microscopy; TGN, *trans*-Golgi network; TIP, tonoplast intrinsic protein; TVP23, Tlg2p-vesicle protein 23; YFP, yellow fluorescent protein; YIP, YPT/RAB-interacting protein.

Introduction

Cell wall secretion is essential for plant cell expansion and growth. Primary cell walls consist of about 20–30% cellulose embedded in a matrix of soluble hemicellulosic and pectic polysaccharides with small amounts of structural and enzymatic proteins (Sandhu et al. 2009, Carpita 2011). While cellulose microfibrils are synthesized by plasma membrane-localized cellulose synthase enzymes, pectins and hemicelluloses are synthesized by Golgi-localized enzymes and secreted to the plasma membrane via secretory vesicles. However, very little is known about the secretion of the soluble polysaccharide matrix of the cell wall (Worden et al. 2012). One of the key limitations in studying soluble cell wall polysaccharides is that unlike proteins, polysaccharides cannot be fluorescently tagged in live cells to follow their biosynthesis and trafficking. Therefore, the analysis of polysaccharide trafficking requires the use of high quality cellular preservation and antibodies specific for polysaccharide epitopes of interest (Zhang et al. 1993, Driouich et al, 1993, Young et al. 2008), or click chemistry (Anderson et al. 2012).

The importance of efficient and targeted post-Golgi vesicle traffic in cell wall secretion has been documented sporadically, since most studies of post-Golgi trafficking have been focused on protein secretion. However, several lines of evidence suggest that chemical or genetic perturbation of the Golgi apparatus and post-Golgi compartments has dramatic effects on cell wall polysaccharide export. Both monensin (a proton ionophore; Boss et al. 1984) and concanamycin A (a V-type H^+-ATPase

Plant Cell Physiol. 54(11): 1867–1880 (2013) doi:10.1093/pcp/pct129, available online at www.pcp.oxfordjournals.org

inhibitor; Huss et al. 2002) upset the proton gradient of the secretory pathway, leading to morphological defects in endomembrane compartments and a decrease in protein secretion (Zhang et al. 1993, Robinson et al. 2004, Dettmer et al. 2006). Interestingly, although monensin causes intracellular accumulation of secreted proteins and hemicelluloses, which are modified in the *trans*-Golgi/*trans*-Golgi network (TGN), it did not affect secretion of pectins (Zhang et al. 1996), implying that several routes of post-Golgi trafficking to the plasma membrane and cell wall may exist.

More recently, molecular genetic studies have corroborated these inhibitor studies and identified several specific targets of these inhibitors. A screen employing secreted green fluorescent protein (secGFP), which does not significantly fluoresce in the apoplast but accumulates in the endomembrane system of secretion mutants, has revealed several Arabidopsis genes required for protein secretion and cell wall synthesis (Zheng et al. 2004). ECHIDNA (ECH) is a protein of unknown function that, based on homology and conserved function between yeast and plants, could act in conjunction with the SYP61–SYP41–VTI12–SNARE [soluble NSF (*N*-ethylmaleimide-sensitive factor) attachment protein receptor] complex to achieve proper targeting of post-Golgi vesicles (Stein et al. 2009, Gendre et al. 2011, Drakakaki et al. 2012). Recently, two YPT/RAB-interacting proteins (YIPs), YIP4a and YIP4b, have been identified as ECH interactors, implying that ECH/YIP4a/YIP4b may recruit RABs for post-Golgi vesicle targeting (Gendre et al. 2013). In *echidna* and *yip4a yip4b* mutants, Golgi function is relatively normal, but TGN morphology and post-Golgi trafficking are defective (Gendre et al. 2011, Gendre et al. 2013). *echidna* mutants also accumulate secGFP and display growth defects (Gendre et al. 2011). The most striking defect of the *echidna* mutant phenotype was disruption of cell wall polysaccharide secretion, resulting in accumulation of pectins in the center of cells that were actively secreting cell wall material, such as hypocotyls and seed coat epidermal cells (Gendre et al. 2013).

Here, a high-resolution study of the *echidna* mutant phenotype was undertaken to determine the location of these polysaccharide accumulations, to characterize the endomembrane defects contributing to this phenotype and to compare polysaccharide and protein traffic. Loss of ECH in seed coat mucilage secretory cells, which are highly specialized for soluble polysaccharide secretion, led to a large accumulation of pectins in the lytic vacuole as marked by γ-tonoplast intrinsic protein (TIP)–GFP. Alterations in the endomembrane system in *echidna* included swellings of the endoplasmic reticulum (ER) that contained both pectin and ER markers. In contrast, protein markers for the TGN and plasma membrane-localized proteins were partially mistargeted to internal multilamellar membranes in *echidna* mutants. These data indicate that ECH is required for proper targeting of pectins to the cell wall, and that in the absence of ECH, pectins accumulate in the vacuole and the ER. Furthermore, the vesicular traffic of polysaccharides and proteins is affected differently in *echidna* mutants, suggesting that different macromolecules are packaged into vesicles leaving the TGN with diverse mechanisms that all require ECH.

Results

Pectins accumulate within *echidna* seed coat mucilage secretory cells

The mucilage secretory cells of the *Arabidopsis thaliana* seed coat epidermis provide a model secretory system in which large amounts of cell wall polysaccharides are secreted as pectic mucilage (Western et al. 2000). In order to determine whether the post-Golgi trafficking mutant *echidna* is defective in seed coat polysaccharide secretion, we employed the ruthenium red assay (Western et al. 2000). When wild-type seeds are incubated in ruthenium red stain, mucilage is released from epidermal cells and a halo of red-stained mucilage surrounds the seed (**Fig. 1A**; Western et al. 2000). This halo was greatly reduced in *echidna* seed coats, indicating a putative defect in mucilage biosynthesis, secretion or release (**Fig. 1A**; Gendre et al. 2013). Scanning electron microscopy (SEM) examination of the seed coat epidermal surface showed that mature wild-type seed coat cells were characterized by raised central columellae, surrounded by a mucilage pocket (**Fig. 1B**). In contrast to the wild type, seed coat cells of *echidna* are severely altered, including flattened or sunken columellae, reduced apoplastic mucilage pockets and abnormal radial cell walls (**Fig. 1B**). The lack of a raised columella and altered mucilage pockets indicate that mucilage production or secretion is defective in *echidna* seeds.

The surface defects observed by SEM were consistent with the phenotype observed in sections of high-pressure frozen, freeze-substituted *echidna* and wild-type seeds examined using light microscopy (**Fig. 1C**; Gendre et al. 2013). During mucilage secretion, wild-type seed coat cells change from typical parenchymous cells to being dominated by a large deposit of polysaccharide on the apical face of the epidermal cells (arrowheads, **Fig. 1C**; Young et al. 2008). Although early epidermal development was similar to that of the wild type, *echidna* mucilage secretory cells had few or no mucilage pockets during mid- and post-secretory stages and contain large accumulations that stained the same color and intensity as extracellular mucilage, inside the center of the cell (**Fig. 1C**). When the inclusions were viewed at high resolution with transmission electron microscopy (TEM), they appeared to be inside the vacuole (**Fig. 2**). Additionally, *echidna* mucilage secretory cells at mid- and post-secretory stages did not display the same polarization of cytoplasmic contents as wild-type cells. In wild-type cells, the large vacuole is positioned at the basal region of the cell, leaving most of the cytoplasm, including amyloplasts, concentrated in the apical cytoplasmic column. In contrast, the vacuole is roughly centered in *echidna* cells, with cytoplasm evenly distributed around it (**Fig. 1C**).

In addition, TEM revealed that in wild-type mucilage secretory cells at the peak of mucilage secretion, Golgi stacks are abundant and are associated with a highly complex TGN, which

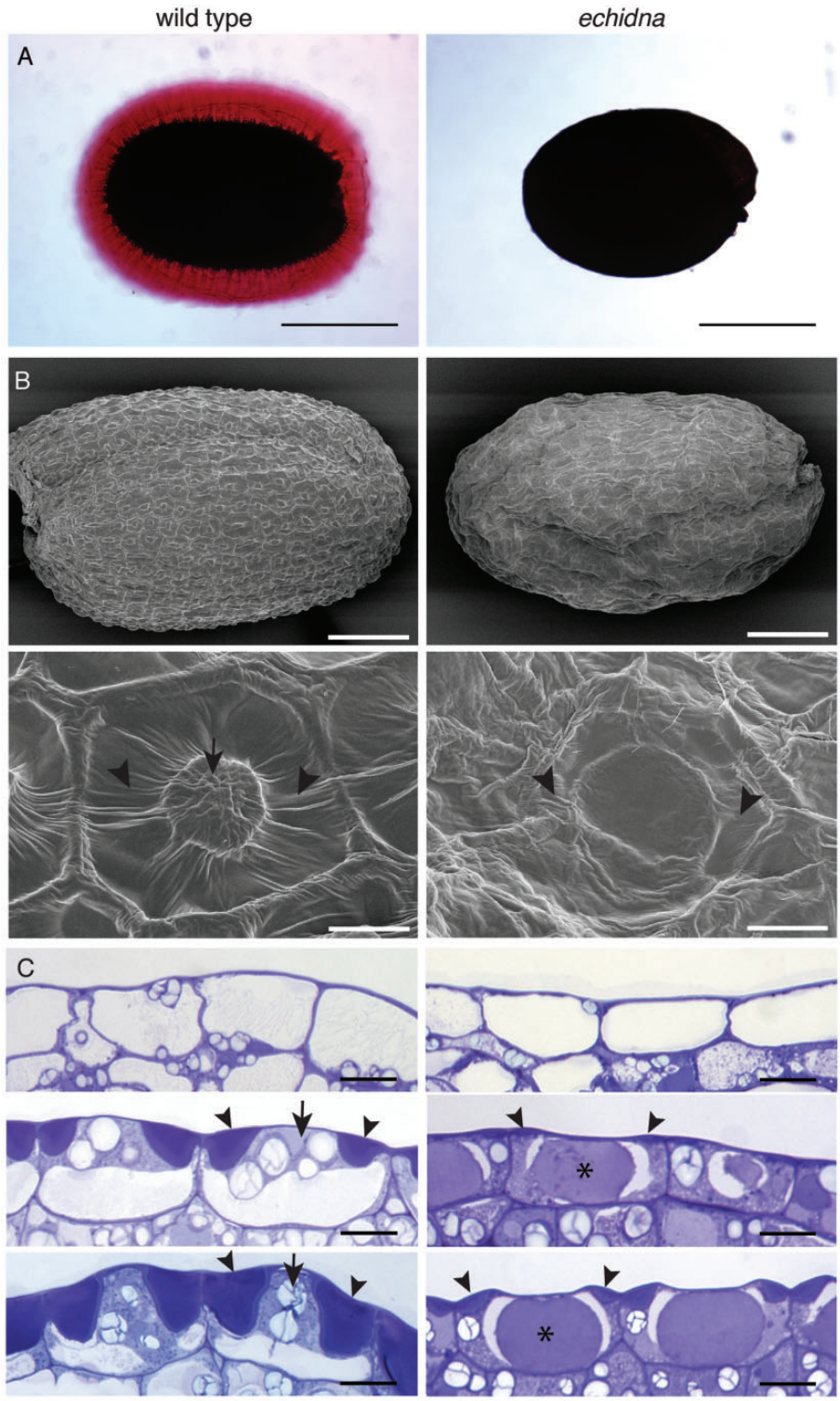

Fig. 1 *echidna* mutants are defective in mucilage deposition. Ruthenium red staining (A) of mature wild-type and *echidna* seeds reveals a mucilage defect upon *echidna* seed coat hydration. Scanning electron micrographs (B) of mature seeds revealed morphological defects in *echidna* seed coats including aberrant mucilage pockets (arrowheads) and a lack of a defined columella that is present in the wild type (arrow). Toluidine blue-stained sections (C) of developing seed coat cells. At the early secretory phase (top), there are no distinguishable differences between the wild type and *echidna*. At mid-secretory phase (middle), mucilage is secreted to the apoplast in the developing mucilage pocket (arrowheads), and the developing columella (arrow) is visible in the wild type. In *echidna* mid-secretory phase cells, only a small amount of mucilage accumulates in the apoplast (arrowheads), and a large accumulation develops in the center of the cell (*). This phenotype persists into post-secretory phase cells (bottom). Scale bars represent 200 μm in A, 100 μm in B (top) and 10 μm in B (bottom) and C.

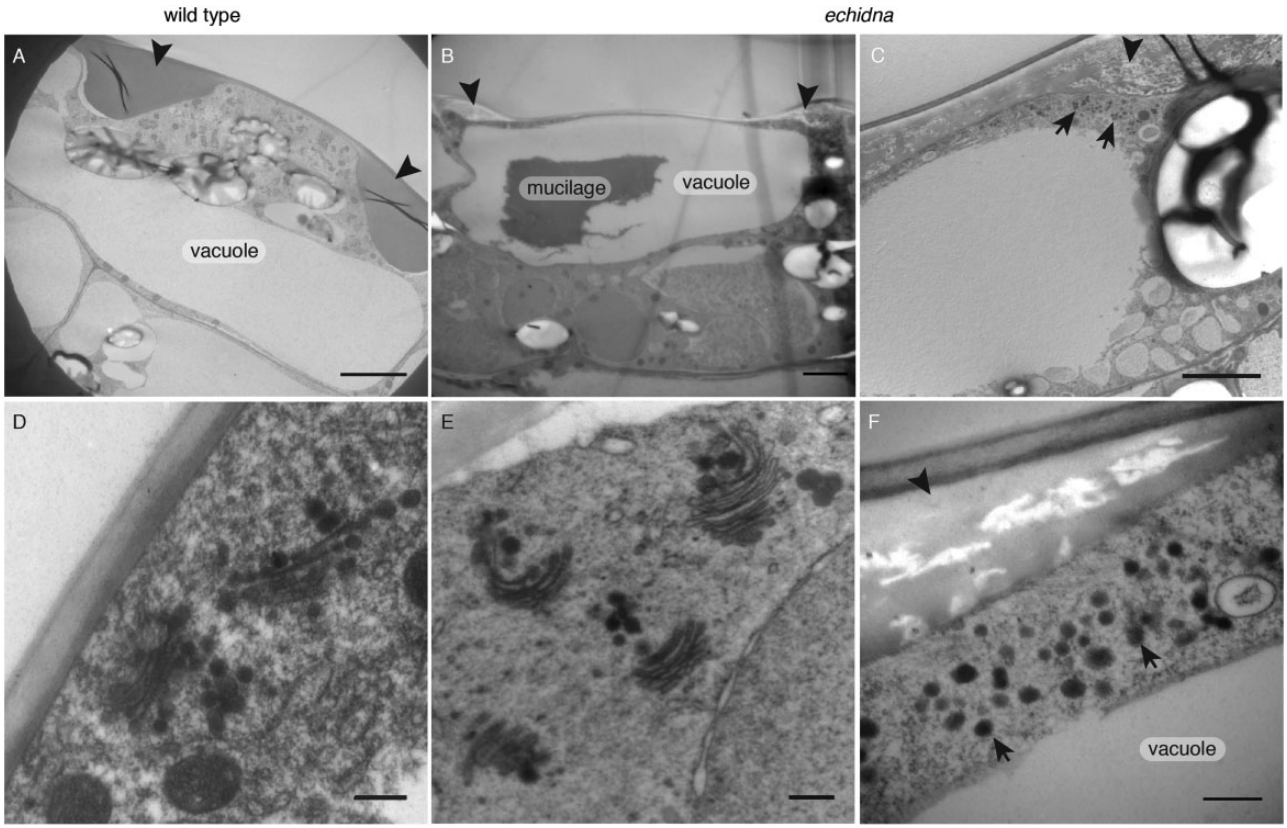

Fig. 2 *echidna* mutants display a variety of subcellular morphology defects. TEM of wild-type seed coat cells (A) shows secreted mucilage in the apical apoplastic space (arrowheads), a large central vacuole and several amyloplasts. TEM of *echidna* seed coat cells (B) reveals only small accumulations of mucilage in the apoplastic space (arrowheads) as well as mucilage in the center of the cell. Compared with wild-type Golgi (D), Golgi are shorter and the TGN appears abnormal in *echidna* (E), and vesicles (arrow) accumulate in a polar fashion near the apical mucilage pocket (arrowhead) (C and F). Scale bars represent 5 μm in and B, and 500 nm in C–F.

develops in correlation with the developmental increase in mucilage synthesis and secretion (**Fig. 2D**; Young et al. 2008). In *echidna* mucilage secretory cells, while the Golgi stacks were intact, the Golgi cisternae were shorter and the TGN contained fewer darkly staining secretory vesicle clusters and was less tightly associated with the Golgi stacks (**Fig. 2E**; Gendre et al, 2011). In addition, there was also an accumulation of darkly staining vesicles in the cytoplasm of *echidna* mucilage secretory cells (**Fig. 2C, F**). In the wild type, dense vesicles contain pectin and are evenly distributed throughout the cytoplasm in mucilage secretory cells (Young et al. 2008). In contrast, dense vesicles accumulate in a polar fashion in *echidna* mutants, with the highest concentration nearest the domain of the plasma membrane adjacent to the mucilage pocket (**Fig. 2F**).

Pectins accumulate within the vacuole of *echidna* cells

To confirm that the accumulations in *echidna* seed coat cells are composed of pectin, sections of seeds at the mid-secretory stage were probed with the anti-seed coat mucilage antibody, CCRC-M36 (Young et al. 2008), which binds to unbranched rhamnogalacturonan I (Pattathil et al. 2010). In the wild type, CCRC-M36 strongly labels the apoplastic mucilage pockets of the mucilage secretory cells, as well as some cytoplasmic puncta, which correspond to the mucilage-producing Golgi stacks, but it does not label any other cell wall material, or anything outside of the mucilage secretory cells (**Fig. 3A**; **Supplementary Fig. S1**). In *echidna* mutants, CCRC-M36 signal was concentrated at the small apoplastic mucilage pockets, but also strongly labeled the center of the cell and cytoplasmic puncta (**Fig. 3A**). This confirmed that the accumulation in the center of *echidna* mutant seed coat cells is mucilage.

To determine the distribution of the pectin in the endomembrane organelles of the seed coat cells in *echidna*, immunoTEM was performed using the CCRC-M36 anti-pectic mucilage antibody. Gold particles conjugated to secondary antibody detected CCRC-M36 epitopes in wild-type mucilage secretory cells in the apoplastic mucilage pocket, the Golgi apparatus, the TGN and secretory vesicles (**Fig. 3B**; see **Supplementary Fig. S2** for controls). In *echidna* mutants, gold particles indicated antibody binding to the Golgi apparatus, the TGN, the small mucilage pockets, as well as the central

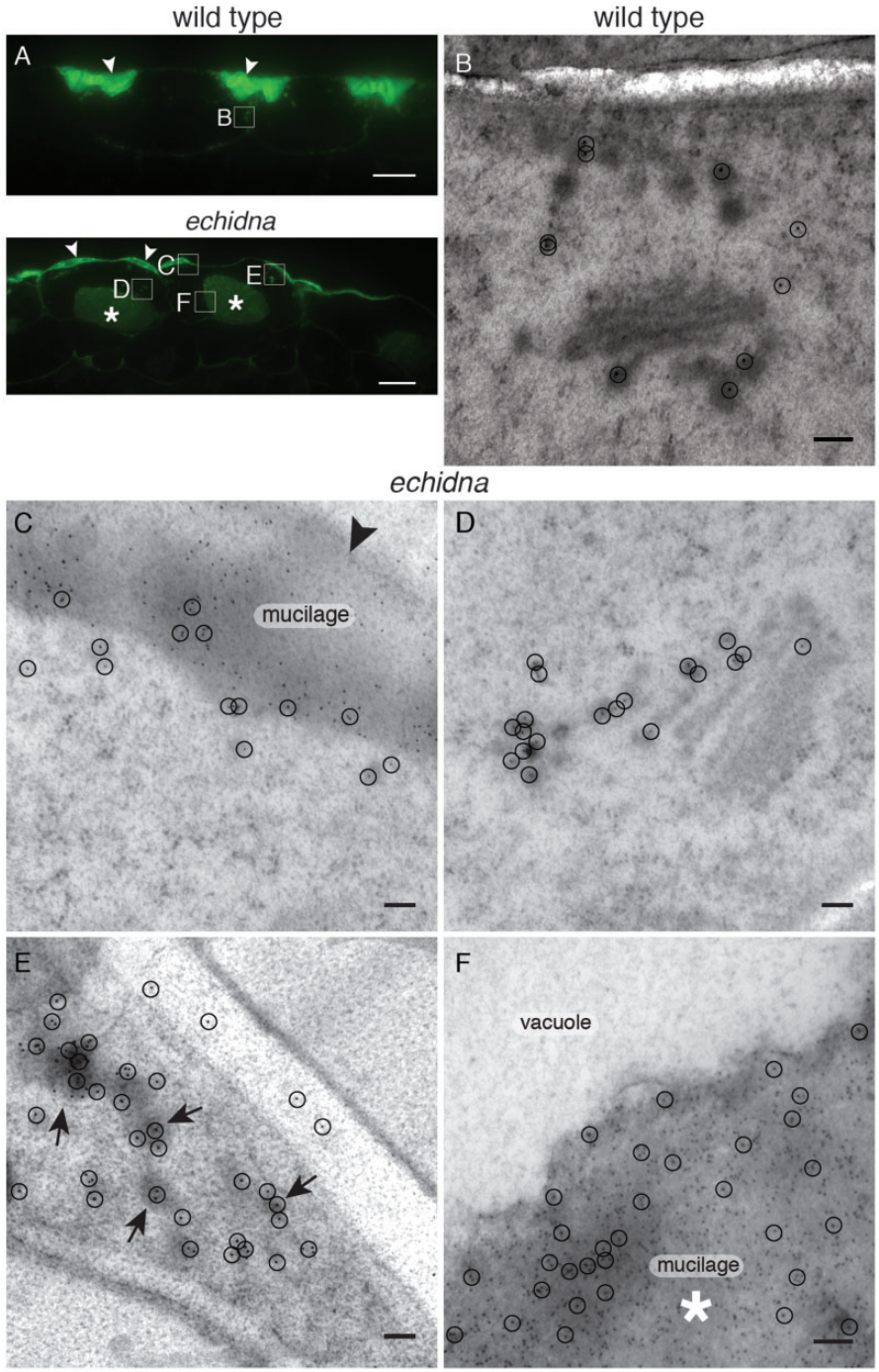

Fig. 3 Mucilage accumulates within *echidna* seed coat cells. Immunofluoresence with the anti-mucilage antibody CCRC-M36 (A) confirms that mucilage accumulates in the apoplast in both the wild type and *echidna* (arrowheads) and also in the center of the cell in *echidna* (*). ImmunoTEM using the CCRC-M36 antibody reveals that mucilage is also localized in the Golgi and TGN in the wild type (B). In *echidna*, mucilage is localized to the apoplast (C), the Golgi and TGN (D), as well as in accumulations of vesicles near the apoplast (E, arrows) and the center of the cell (F). Squares in A and B indicate areas within the cells where TEM images were taken for B-F. Scale bars represent 10 μm in A and B, and 200 nm in B–F; representative gold particles in B–F are highlighted by circles.

mucilage accumulation, and putative ER bodies (**Fig. 3**; controls in **Supplementary Fig. S2**). Additionally, CCRC-M36 signal was detected in the vesicles that accumulate near the apical plasma membrane in *echidna* seed coat cells (**Fig. 3E**), implying that secretory vesicles containing pectin can form properly in *echidna* but they cannot properly fuse with their target membrane. The anti-pectic mucilage antibody did not significantly label the pre-vacuolar compartment/multivesicular bodies.

Although mucilage was clearly mistargeted in *echidna* mutants, the nature of the compartment containing mucilage was not known. Since this mucilage appeared to accumulate in the central lytic vacuole, the tonoplast fluorescent protein marker γ-TIP–GFP (Boursiac et al. 2005) was crossed into *echidna* mutants and visualized with confocal microscopy. In both wild-type and *echidna* seed coat cells at the mid-secretory stage, γ-TIP–GFP labeled the tonoplast, which outlined the lytic vacuole around the periphery of the cell, including where the vacuole was pushed inwards by amyloplasts, which are visible in brightfield (**Fig. 4A**). ImmunoTEM confirmed that anti-γ-TIP (Jauh et al. 1999) labeled the tonoplast and the periphery of the mucilage accumulation in *echidna* mutants (**Fig. 4B**). These data verify that mucilage, which is synthesized but not secreted in *echidna* mutants, accumulates in the central lytic vacuole.

Pectins also accumulate within ER bodies of *echidna* cells

TEM of *echidna* mutants also revealed unusual endomembrane compartments, which resembled ER dilations. Therefore, the ER marker GFP–HDEL (Batoko et al. 2000) was used to determine whether there were ER morphology changes in *echidna* mutants. In contrast to the wild-type cell, where ER was confined to an even reticulum around the cell cortex, *echidna* mutant ER displayed many dilations that correspond in size, shape and relative frequency to the ER bodies observed in TEM (**Fig. 5A**). In TEM preparations that were optimized for morphology, the ER structures of wild-type and *echidna* (**Fig. 5B**) were compared. Compartments of 300–1,500 nm diameter that were surrounded by ribosomes were observed exclusively in *echidna*. In some planes of section, direct connections to the ER were seen (**Fig. 5B**), indicating that they are ER-derived bodies. These ER bodies are morphologically distinct from oil or protein storage bodies found in embryos, or ER bodies typically found in leaf and root epidermal cells (Hayashi et al. 2001, Herman 2008). ImmunoTEM using CCRC-M36 confirmed that pectins accumulate in these ER bodies (**Fig. 6A**), and anti-calreticulin (an ER marker; Coughlan et al. 1997) confirmed the ER origin of these structures (**Fig. 6B**). Together, these results demonstrate that loss of normal ECH-mediated vesicle traffic has broad impacts on anterograde cell wall polysaccharide cargo secretion, with pectin cargo inappropriately accumulating, directly or indirectly, in both the vacuole and ER bodies.

Pectins and membrane proteins accumulate in distinct compartments in *echidna* mutants.

Our data demonstrated severe consequences of loss of function of *ECHIDNA* for polysaccharide secretory vesicle traffic. This raised the question of whether similar consequences would be seen for TGN resident proteins and for cargo proteins destined for the plasma membrane. Given that distinctive morphological changes occur to the TGN in seed coat cells during mucilage secretion (Young et al. 2008), the localization of the TGN marker SYP61–cyan fluorescent protein (CFP) (Robert et al. 2008) was examined in live cells of wild type and *echidna* mutants. In wild-type secretory phase seed coat cells, SYP61–CFP was localized to abundant puncta throughout the cytoplasm (**Fig. 7A**). In *echidna* secretory phase seed coat cells, this TGN marker was localized to a few puncta, and also strongly labeled circular membrane inclusions (arrowheads, **Fig. 7A**). In TEM, multilamellar membrane structures of 2–5 μm in diameter were observed and resembled pre-autophagy structures or autophagosomes (**Fig. 7C**). Similar fluorescent membrane inclusions were observed in the seed coat cells expressing γ-TIP–GFP (**Fig. 4A**), and immunoTEM with anti-γ-TIP confirmed that this vacuolar marker is localized to the multilamellar membrane structures (**Fig. 7E**) in addition to the signal detected at the tonoplast (**Fig. 4B**). Interestingly, these multilamellar structures in which proteins accumulated did not label positively for pectin when tested with the CCRC-M36 antibody (**Fig. 7F**).

Previous characterization of the TGN and secretion defects in *echidna* root cells has demonstrated that the TGN-localized H^+-ATPase subunit, VHA-a1, is mislocalized to circular puncta (Gendre et al. 2011), which correspond in size and morphology to the multilamellar membrane structures observed in *echidna* seed coat cells. In order to test whether mucilage mislocalization in *echidna* mutants could be due to VHA-a1 mislocalization, VHA-a1–GFP (Dettmer et al. 2006) was examined in *echidna* mutants. In wild-type secretory phase seed coat cells, VHA-a1–GFP was localized to abundant puncta throughout the cytoplasm, corresponding to the TGN. In *echidna*, VHA-a1–GFP signal was primarily localized to these puncta, with some mislocalization to the multilamellar membrane aggregations (**Supplementary Fig. S3A**, **B**). To test whether this mild VHA-a1–GFP mislocalization affects mucilage secretion, *VHA-a1* levels were down-regulated using ethanol-inducible RNA interference (RNAi)-VHA-a1 lines, and this was confirmed by reverse transcription–PCR (RT–PCR) (**Supplementary Fig. S3C**; Brüx et al. 2008). Seeds induced during the pre- to post-secretion stages of seed development were screened using the ruthenium red assay (Western et al. 2000), and showed no discernible defects in mucilage release, compared with the wild type (**Supplementary Fig. S3**). These data suggest that the mislocalization of VHA-a1 in *echidna* is not responsible for the mislocalization of pectin, and that *echidna* plays a direct role in the proper trafficking of pectin cargo.

To test the traffic of a plasma membrane-localized protein, yellow fluorescent protein (YFP)–ABCG11, an ATP-binding cassette transporter that is required for wax and cutin secretion (Bird et al. 2007), was observed in mid-secretory phase seed coat cells. In the wild type, YFP–ABCG11 signal was confined to the plasma membrane of seed coat secretory cells (**Fig. 7B**). In *echidna* mutants, YFP–ABCG11 was primarily detected at the plasma membrane; however, there was also some YFP–ABCG11 accumulation in the circular membrane accumulations, as observed with γ-TIP–GFP and SYP61–CFP (arrowheads, **Fig. 7B**). Since, in this system, YFP–ABG11 was ectopically expressed with the 35S promoter, specific antibodies against another plasma membrane protein, aquaporin

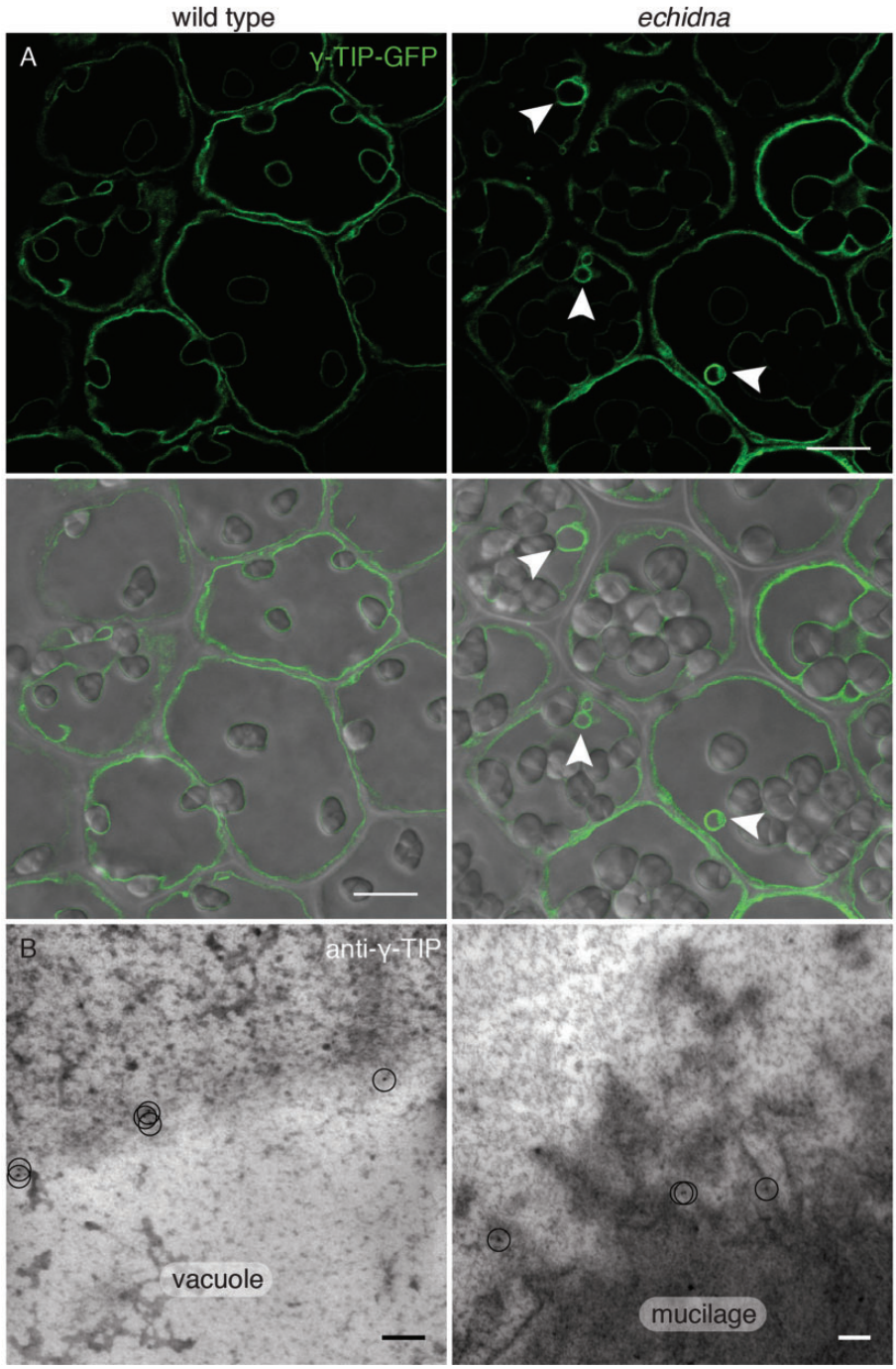

Fig. 4 Mucilage accumulates in the central vacuole in *echidna* mutants. Confocal microscopy of the vacuole marker γ-TIP–GFP (A) reveals that in wild-type cells γ-TIP–GFP (top) is localized to the central vacuole, which is deformed around the amyloplasts visible in the brightfield image (bottom). γ-TIP–GFP is localized to the vacuole in *echidna* mutants, but also strongly labels a circular structure (arrowheads) that does not co-localize with any of the amyloplasts. ImmunoTEM using anti-γ-TIP (B) confirms γ-TIP localization to the tonoplast in the wild type, and demonstrated that the mucilage accumulation in the center of *echidna* cells is surrounded by the tonoplast. Scale bars represent 10 μm in A and 200 nm in B; gold particles in B are highlighted by circles.

PIP2 (plasma membrane intrinsic protein 2) (Bots et al. 2005), were employed. Anti-PIP2 specifically labeled the plasma membrane in wild-type cells, but in *echidna* mutants, anti-PIP2 was found primarily in the large, circular membrane accumulations, as well as at low levels in the plasma membrane and in the tonoplast (**Fig. 7D**). These data indicate that the circular multilamellar membrane inclusions contain TGN, tonoplast and plasma membrane proteins, but not mucilage. These data

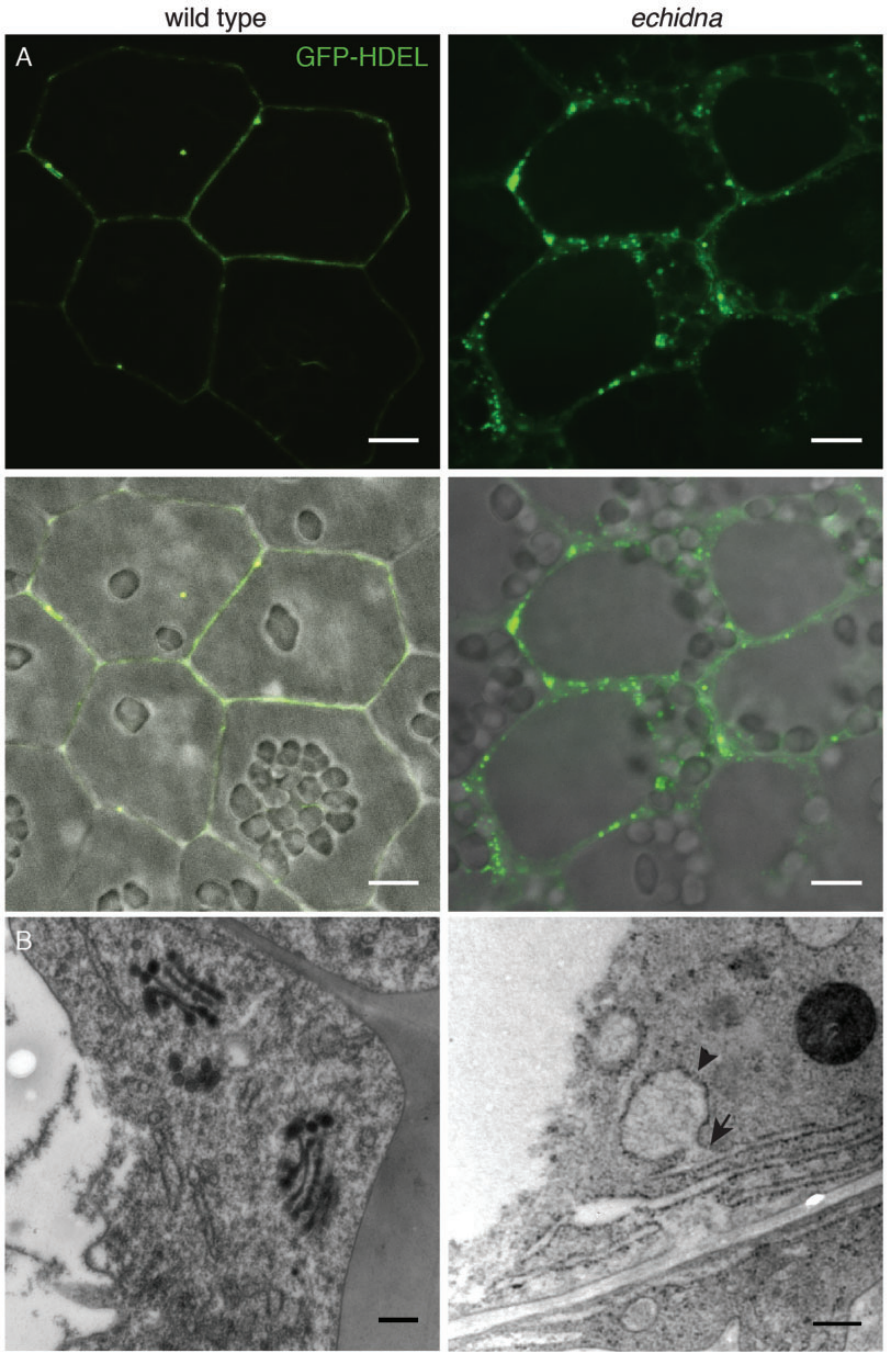

Fig. 5 *echidna* mutants display defects in ER morphology. Confocal microscopy of the ER marker GFP–HDEL (A) (top) reveals a typical reticulate ER network in wild-type cells that is pushed to the edge of the cells, as visible in brightfield microscopy (bottom). GFP–HDEL is localized to the ER network in *echidna* mutants, but also strongly labels puncta throughout the cytoplasm. In TEM (B), these punctae appear to be ER dilations (arrowheads) which are not present in the wild type and appear to be directly connected to the ER (arrow). Scale bars represent 10 μm in A and 500 nm in B.

also suggest that post-Golgi trafficking of soluble cell wall polysaccharides is distinct from post-Golgi trafficking of these membrane proteins in *echidna* mutants, which suggests that different post-Golgi mechanisms exist that are affected to varying degrees in *echidna* mutants.

Discussion

In this study, the seed coat phenotype of the *echidna* mutant provided a rare opportunity to observe the perturbation of cell wall vesicle trafficking during a developmental period of

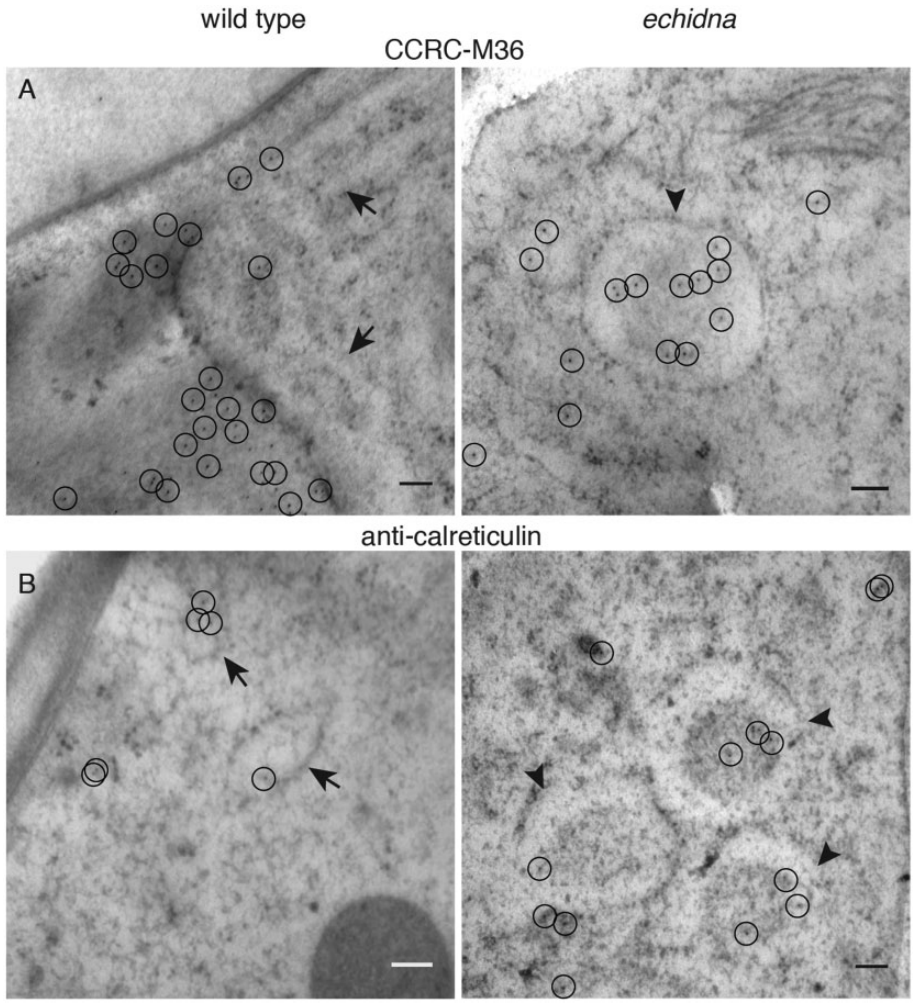

Fig. 6 ImmunoTEM reveals that mucilage is mislocalized to ER dilations in *echidna*. ImmunoTEM using CCRC-M36 (A) reveals that while mucilage does not accumulate in the ER of the wild type (arrows), mucilage is present in the ER dilations in *echidna* (arrowheads). ImmunoTEM using anti-calreticulin (B) that labels the ER in the wild type confirms that these mucilage-containing structures in *echidna* are ER derived (arrowheads). Scale bars represent 200 nm; representative gold particle are highlighted by circles.

abundant pectin secretion. The loss of function of ECH had dramatic effects on efficient cell wall polysaccharide export (**Fig. 8**). Rather than pectin being secreted to the apical domain of the plasma membrane surrounding the cytoplasmic column, as is the case in the wild type (**Fig. 8A**), pectin was found in the central vacuole and, to a lesser extent, in ER bodies in *echidna* (**Fig. 8B**). Accumulations of dense vesicles that labeled with the anti-pectin CCRC-M36 antibody at the cell cortex, adjacent to the usual site of secretion, indicate that vesicles did not dock or fuse efficiently at their usual target membrane in *echidna*, although the small apoplastic mucilage pockets present do suggest that a small number of vesicles were still able to target, dock and fuse with their target membrane. These successful vesicles could represent a population that contained the appropriate post-Golgi secretory vesicle identity, including the correct suite of vesicle traffic machinery, e.g. RABs and SNAREs. Thus, it appears that the primary defect in the *echidna* mutant is that the majority of secretory vesicles no longer efficiently traffic to or fuse with the plasma membrane, suggesting a role for ECH in targeting dense secretory vesicles carrying cell wall polysaccharides to the correct destination, probably by recruiting the appropriate vesicle trafficking proteins such as RABs and SNAREs at the TGN.

ECH is homologous to the yeast TGN-localized protein, TVP23 (Tlg2p-vesicle protein 23), which genetically interacts with a *trans*-Golgi SNARE complex and acts in retrograde trafficking (Stein et al. 2009). Yeast mutants that are defective in TVP23 display accumulation of a recycled protein in early endosomes, which is indicative of a defect in early endosome to TGN trafficking (Stein et al. 2009). Interestingly, expression of Arabidopsis ECH cDNA in Δtvp23Δypt6 yeast was able to rescue fully the growth phenotype (Gendre et al. 2011), and immunological isolation and proteomics of SYP61-positive TGN/vesicles from Arabidopsis detected ECH in the same vesicles as the *trans*-Golgi SNARE SYP61 (Drakakaki et al. 2012), suggesting conservation of function between yeast and plants.

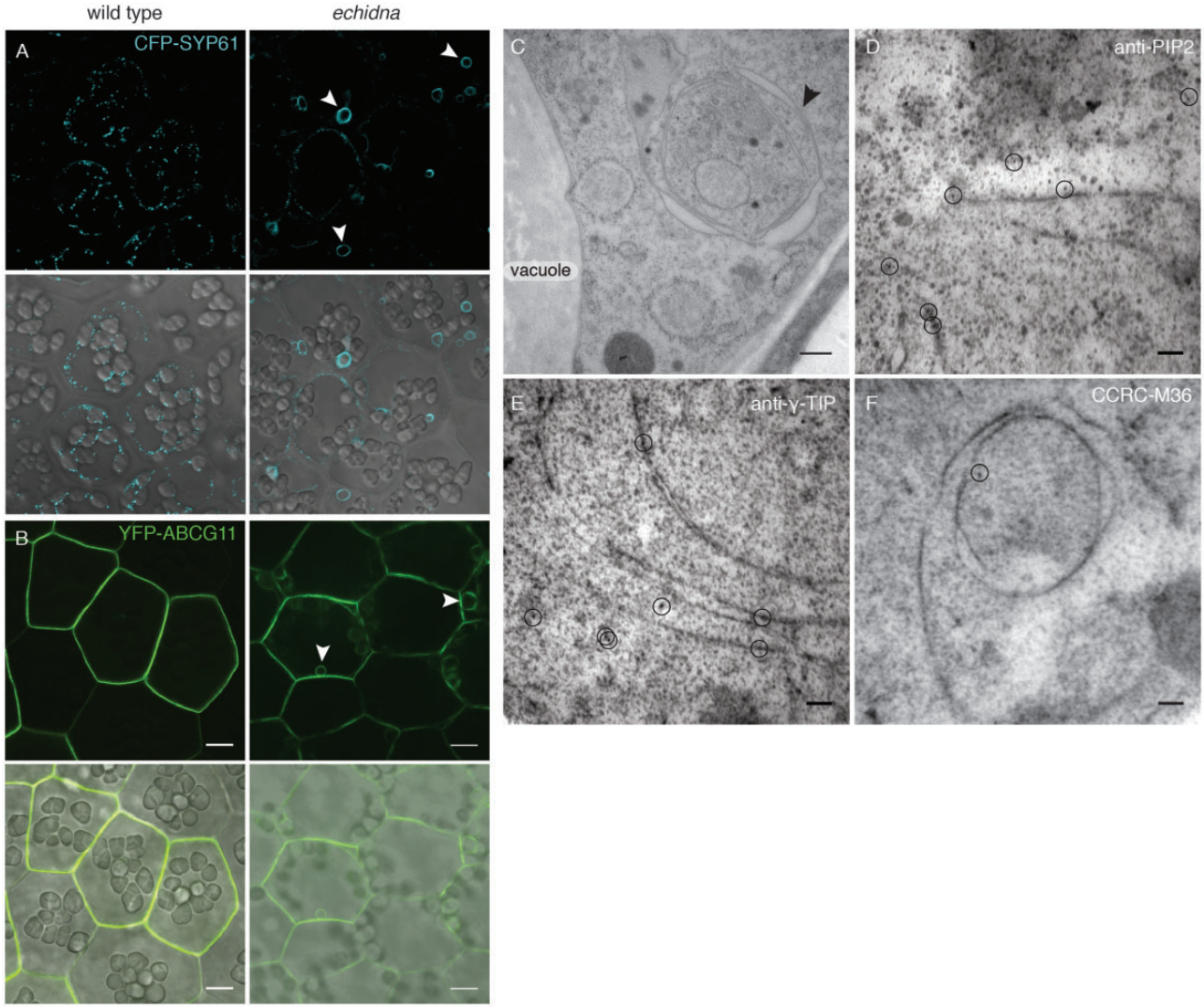

Fig. 7 TGN and plasma membrane proteins accumulate in compartments distinct from mucilage accumulation in *echidna* mutants. TGN-localized SYP61–CFP (A) is partially mislocalized to circular structures in *echidna* that are distinct from amyloplasts. This is also true for the plasma membrane-localized YFP–ABCG11 (B). TEM reveals that these circular structures are multilamellar (C). ImmunoTEM using anti-PIP2 (D) and anti-γ-TIP (E) confirms the presence of mislocalized plasma membrane and vacuole proteins, respectively, in these structures. However, immunoTEM using CCRC-M36 (F) reveals that mucilage is not mislocalized to these compartments. Scale bars represent 10 μm in A and B, 500 nm in C and 200 nm in D–F; representative gold particles in D–F are highlighted by circles.

Furthermore, the recent characterization of YIP4 proteins (RAB-interacting proteins) as interacting partners with TVP23 in yeast (Inadome et al. 2007) and ECH in plants (Gendre et al. 2013) strengthens the conservation of function. By analogy to yeast, it is possible that breakdown in post-Golgi trafficking in *echidna* mutants could result from altered retrograde traffic between the endosome and the TGN. However, the endomembrane phenotypes of yeast and Arabidopsis *echidna* mutants are distinct, suggesting that ECH may have evolved alternative or additional roles in cell wall secretion in plants.

One of the major concerns of working with a protein of unknown function is that mutant phenotypes include both primary and secondary defects. For example, the TGN-localized H^+-ATPase, VHA-a1, is mislocalized in root cells of *echidna* (Gendre et al. 2011), which may disrupt the proton gradients that help to maintain the identity of endomembrane compartments (Dettmer et al. 2006, Brüx et al. 2008). However, mislocalization of GFP–VHA-a1 was minimal in *echidna* seed coat cells, and seeds in which RNAi-VHA-a1 (Brüx et al. 2008) had been induced showed no defect in mucilage release. This suggests that the loss of ECH, and not the mislocalization of VHA-a1, may cause the defects in cell wall secretion.

Whatever the underlying primary defect in secretory vesicle function in *echidna* mutants, the unexpected result was the steady-state accumulation of pectin in the central vacuole. This could be due to either a stress response to vesicle accumulation or the problems with post-Golgi vesicle identity leading to direct fusion of vesicles with the tonoplast. It is possible

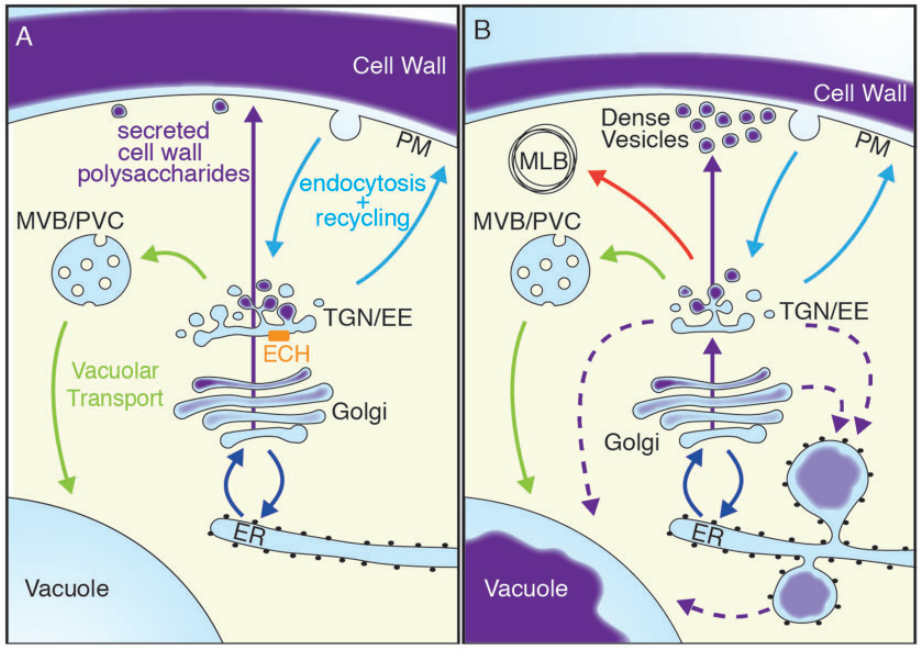

Fig. 8 Overview of the phenotypes observed in *echidna* seed coat cells. At the height of mucilage secretion in wild-type seed coat cells (A), the *trans*-Golgi network (TGN)-localized ECHIDNA is required for secretion of large amounts of Golgi-synthesized pectic mucilage (purple) via secretory vesicles. The TGN also acts as an early endosome (EE) by receiving endocytic material, which may be recycled to the plasma membrane (PM) or transported to the vacuole via a multivesicular body/pre-vacuolar compartment (MVB/PVC). In the *echidna* mutant (B), vacuolar transport and endocytosis remain largely unaffected, but the TGN loses its ability to generate competent vesicles for wild-type levels of mucilage secretion. This results in the polar accumulation of dense, polysaccharide-containing vesicles near the PM, as well as mucilage accumulation in the endoplasmic reticulum (ER) and the vacuole. Membrane proteins targeted to the PM and the tonoplast (including ABCG11, PIP2, γ-TIP and SYP-61) are partially mislocalized to multilamellar bodies (MLBs) that do not contain any mislocalized polysaccharides.

that mucilage may reach the vacuole by autophagy, which would serve to sequester the mucilage and reclaim the vesicle membranes and targeting proteins. Unfortunately, due to the difficulties in imaging established markers for autophagy such as GFP–ATG8e or monodanslycadaverine (MDC) (Contento et al. 2005) in the seed coat, we were unable to determine whether autophagic compartments are up-regulated in *echidna*. Pectin also accumulated in the ER bodies in less dense aggregates than in the vacuole in *echidna* mutants. Pectin mislocalization to the ER bodies may be a secondary defect of the post-Golgi trafficking issues in *echidna* mutants (Gendre et al. 2011). Although the Golgi apparatus is still morphologically distinct from the ER in *echidna* mutants, it is possible that the endomembrane disorganization observed in *echidna* mutants is also causing leakage of Golgi cargo (i.e. mucilage) or Golgi-resident enzymes (i.e. glycosyl transferases and associated nucleotide sugar transporters) to the ER, resulting in mucilage accumulation in ER dilations. The pectin in ER bodies may also contribute to the vacuolar accumulations of pectin, and direct delivery to the vacuole from the ER cannot be excluded.

Interestingly, secreted plasma membrane proteins and secreted polysaccharide cargo within *echidna* cells accumulate in distinct places within the cell. While pectic polysaccharides accumulated in the vacuole and the ER bodies, plasma membrane proteins ABCG11 and PIP2 accumulated in large multilamellar membrane accumulations that also contained the TGN/post-Golgi SNARE, SYP61, and the tonoplast marker γ-TIP. These structures could represent precursors to autophagosomes or protein aggregates similar to those seen in nutrient-starved tobacco BY-2 cells (Toyooka et al. 2009, Takatsuka et al. 2011). Because cell wall polysaccharides and transmembrane plasma membrane proteins are mislocalized to distinct compartments in *echidna* mutants, these data suggest that, although both cargo types are secreted to the plasma membrane, they may travel in vesicles with distinct trafficking machinery, or that the plasma membrane proteins are recycled through the TGN/early endosome in an ECH-dependent manner. These data corroborate previous results that found that the dominant-negative version of the SYP121 SNARE caused a decrease in secretion of soluble protein markers β--glucuronidase (GUS) and secGFP, but had no effect on either a secreted glycosylphosphatidylinositol (GPI)-anchored protein (De Caroli et al. 2011) or secreted polysaccharides (Leucci et al. 2007). These results highlight the complexity of the plant endomembrane trafficking network since different cargoes destined to the same target may be transported in different pathways, using different sets of vesicular trafficking machinery and/or targeting motifs.

In summary, we have shown here that secretion of non-cellulosic cell wall components to the plasma membrane

requires ECH-dependent machinery for efficient trafficking. In the absence of this proper machinery, these soluble cell wall cargoes are mislocalized to the vacuole and the ER, either directly, through vesicle fusion, or indirectly, through autophagy or improper retrograde trafficking. The mislocalization of membrane-localized proteins and soluble cargo in *echidna* emphasizes the importance of studying polysaccharide traffic, in addition to protein trafficking, in order to form a complete understanding of cell wall synthesis and secretion.

Materials and Methods

Plant material

Arabidopsis thaliana seeds were sown on AT media plates (Haughn and Somerville 1986) and grown at 21°C, 70–80% humidity and constant light (~100 μE m^{-2} s^{-1}) in an environmental growth chamber (Conviron). After 10–14 d, seedlings were transferred to Sunshine mix 5 soil and returned to the same growth conditions. To obtain seeds at different stages in development, siliques were marked with non-toxic paint at the day of anthesis, according to Western et al. (2000). Because of general developmental defects in *echidna* mutants, it was difficult to obtain accurately developmentally staged seeds according to established convention of days post-anthesis (dpa; Western et al. 2000). Therefore, *echidna* mutant seeds were grouped into three stages: pre-secretion (similar to the wild type 4 dpa, before mucilage accumulation has begun), mid-secretion (similar to the wild type 7 dpa, at which time mucilage synthesis and secretion is at its peak) and post-mucilage secretion (similar to the wild type 10 dpa, at which time mucilage synthesis and secretion has finished and secondary cell wall synthesis has begun).

To induce RNAi-VHA-a1 lines (Brüx et al. 2008), small incisions were made on pre-secretory siliques of both wild-type and ethanol-inducible RNAi-VHA-a1. Siliques were then immersed in 5% ethanol and were re-immersed once a day for 6 d to ensure that induction was occurring throughout the duration of mucilage secretion. Seeds were allowed to grow to maturity, collected, and screened using the ruthenium red staining assay. Plant genotypic lines *echidna* (SAIL_163_E09) mutants in the Col-0 background (Gendre et al. 2011), *abcg11-3* (Col-0 background) + 35S::YFP-ABCG11 (Bird et al. 2007), Col-0 + 35S::GFP-HDEL were a gift from H. Zheng at McGill University (Batoko et al. 2000). pSYP61::SYP61-CFP (Robert et al. 2008) was a gift from N. Raikhel, pVHA-a1::VHA-a1-GFP (Dettmer et al. 2006) and pAlcA::VHA-a1RNAi (Brüx et al. 2008) were a gift from K. Schumacher. 35S::γ-TIP-GFP (Boursiac et al. 2005) was a gift from C. Maurel. Crosses were genotyped using the primers indicated in **Supplementary Table S1**.

Gene expression analysis

Seed coats from mid-secretory phase seeds were isolated from the embryo and quickly frozen with liquid nitrogen. RNA was isolated using the RNAqueous-Micro kit (Ambion). cDNA was synthesized using 1 μg of RNA using a mixed oligo dT15, dT17 and dT20 primer set and M-MLV reverse transcriptase (Promega). RT–PCR was performed for 29 cycles using 5 μl of cDNA with intron-flanking, gene-specific primers for *VHA-a1* (see **Supplementary Table S1**). The *UBC10* ubiquitin-conjugating enzyme was used as the loading control. PCR products were visualized using SYBR-Safe (Invitrogen).

Ruthenium red staining

Mature seeds were incubated in 0.01% (w/v) aqueous solution of ruthenium red for 30 min at room temperature under gentle shaking. Seeds were then mounted in water and viewed using a Leica DMR microscope equipped with a QICAM digital camera (QIMAGING).

Scanning electron microscopy

Mature seeds were dry mounted on stubs and coated with 10 nm of palladium–gold using a Cressington 208HR sputter coater. Samples were viewed on a Hitachi S4700 FE-SEM with an accelerating voltage of 5 kV, beam current of 10 μA and a working distance of 12 mm, using a mix of both the upper and lower detectors.

Confocal microscopy

Mid-secretory phase seeds were mounted in water and viewed under a Leica DMI6000 B inverted microscope with a Perkin Elmer spinning-disk scan head. YFP–ABCG11 was detected using the 514 nm laser diode and 540/30 nm emission filters. GFP–HDEL was detected using the 488 nm laser diode and 525/36 nm emission filters. SYP61–CFP, VHA-a1–GFP and γ-TIP–GFP were viewed under an axioplan inverted microscope with a Zeiss LSM 780 spectral CLSM system. γ-TIP–GFP and VHA-a1–GFP were detected using the 488 nm laser and 493–598 nm emission filters. SYP61–CFP was detected with the 405 nm laser and 454–581 nm emission filters.

High-pressure freezing, TEM and immunogold labeling

Staged seeds were high-pressure frozen in 1-hexadecene in B-type sample holders (Ted Pella) using a Leica HPM-100. For morphology, freeze substitution in 2% osmium tetroxide and 8% dimethoxypropane, resin infiltration with Spurr's resin, sectioning, and post-staining with 2% uranyl acetate and lead citrate were performed as described in McFarlane et al (2008). For immunolabeling, high-pressure frozen samples were freeze-substituted in 0.1% uranyl acetate, 0.25% glutaraldehyde and 8% dimethoxypropane, then infiltrated with LR White resin (London Resin Company), as described in McFarlane et al. (2008). Immunolabeling was performed according to McFarlane et al. (2008). For immunoTEM, primary antibodies were 1/10 M36 (generated in mouse against seed coat mucilage from the Complex Carbohydrate Research Center, University of Georgia; Pattathil et al. 2010), 1/20 polyclonal anti-calreticulin [generated in rabbit against Castor bean (*Ricinus communis*

L. cv. Hale) calreticulin; a gift from Dr. Sean Coughlan; Coughlan et al. 1997], 1/20 anti-γ-TIP (generated in rabbit against the conserved C-terminal domain of γ-TIP; a gift from Dr. John Rogers; Jauh et al. 1999) and 1/50 polyclonal anti-PIP2 [generated in rabbit against tobacco (*Nicotiana tabacum* cv. Petit Havana SR1) PIP2; a gift from Dr. Ralf Kaldenhoff; Bots et al. 2005). Secondary antibodies were 1/100 goat anti-mouse or 1/100 goat anti-rabbit conjugated to 10 nm gold (Ted Pella). Samples were viewed using a Hitachi 7600 transmission electron microscope at 80 kV accelerating voltage with an ATM Advantage HR digital CCD camera (Advanced Microscopy Techniques).

Immunofluorescence

Samples were staged, high-pressure frozen, freeze-substituted in glutaraldehyde and uranyl acetate, and embedded in LR White resin as for immunoTEM (above). Thick sections (250 nm) were prepared using a Leica Ultracut UCT Ultramicrotome and placed on Teflon-coated glass slides (Electron Microscopy Sciences). The morphology of each sample was surveyed using 1% toluidine blue in 1% sodium borate using a Leica DMR Microscope. New sections were processed for immunofluorescence as described in Young et al. (2008). Briefly, slides were incubated in a blocking solution containing of 2.5% bovine serum albumin in Tris-buffered saline (TBS) with 0.1% Tween. After washing with TBS, samples were incubated with 1/10 CCRC-M36 (generated in mouse against seed coat mucilage from the Complex Carbohydrate Research Center, University of Georgia; Pattathil et al. 2010) for 1 h at room temperature. Sections were washed with TBS and then incubated in 1/100 goat anti-mouse secondary antibody conjugated to Alexa488 (Molecular Probes). Sections were washed again with TBS followed by distilled water and viewed under a Leica DMR Microscope equipped with a ebq100 mercury fluorescent source with a 450–490 nm band pass excitation filter and no emission filter (Leica), and a QICAM digital camera (QIMAGING).

Supplementary data

Supplementary data are available at PCP online.

Funding

This work was supported by the Canadian Natural Sciences and Engineering Research Council [Discovery and CREATE to A.L.S., G.W.H., CGS D3-347686-008 to H.M.]; The Swedish Research Council Formas and Swedish University of Agricultural Sciences [to R.P.B.]

Acknowledgments

We thank the University of British Columbia Bioimaging Facility for technical assistance, and Robin Young, Jonathan Griffiths and Teagen Quilichini for helpful discussions and comments on the manuscript.

Disclosures

The authors have no conflicts of interest to declare.

References

Anderson, C., Wallace, I. and Somerville, C. (2012) Metabolic click-labeling with a fucose analog reveals pectin delivery, architecture, and dynamics in Arabidopsis cell walls. *Proc. Natl Acad. Sci. USA* 109: 1329–1334.

Batoko, H., Zheng, H.Q., Hawes, C. and Moore, I. (2000) A RAB1 GTPase is required for transport between the endoplasmic reticulum and Golgi apparatus and for normal Golgi movement in plants. *Plant Cell* 12: 2201–2218.

Bird, D., Beisson, F., Brigham, A., Shin, J., Greer, S., Jetter, R. et al. (2007) Characterization of Arabidopsis ABCG11/WBC11, an ATP binding cassette (ABC) transporter that is required for cuticular lipid secretion. *Plant J.* 52: 485–498.

Boss, W.F., Morre, D.J. and Mollenhauer, H.H. (1984) Monensin-induced swelling of Golgi apparatus cisternae mediated by a proton gradient. *Eur. J. Cell Biol.* 34: 1–8.

Bots, M., Feron, R., Uehlein, N., Weterings, K., Kaldenhoff, R. and Mariani, T. (2005) PIP1 and PIP2 aquaporins are differentially expressed during tobacco anther and stigma development. *J. Exp. Bot.* 56: 113–121.

Boursiac, Y., Chen, S., Luu, D., Sorieul, M., van den Dries, N. and Maurel, C. (2005) Early effects of salinity on water transport in Arabidopsis roots: molecular and cellular features of aquaporin expression. *Plant Physiol.* 139: 790–805.

Brüx, A., Liu, T.Y., Krebs, M., Stierhof, Y.D., Lohmann, J.U., Miersch, O. et al. (2008) Reduced V-ATPase activity in the trans-Golgi network causes oxylipin-dependent hypocotyl growth inhibition in Arabidopsis. *Plant Cell* 20: 1088–1100.

Carpita, N.C. (2011) Update on mechanisms of plant cell wall biosynthesis: how plants make cellulose and other (1→4)-β-D-glycans. *Plant Physiol.* 155: 171–184.

Contento, A.L., Xiong, Y. and Bassham, D.C. (2005) Visualization of autophagy in arabidopsis using the fluorescent dye monodansylcadaverine and a GFP–AtATG8e fusion protein. *Plant J.* 42: 598–608.

Coughlan, S.J., Hastings, C. and Winfrey, R. Jr (1997) Cloning and characterization of the calreticulin gene from *Ricinus communis* L. *Plant Mol. Biol.* 34: 897–911.

De Caroli, M., Lenucci, M.S., Di Sansebastiano, G., Dalessandro, G., De Lorenzo, G. and Piro, G. (2011) Protein trafficking to the cell wall occurs through mechanisms distinguishable from default sorting in tobacco. *Plant J.* 65: 295–308.

Dettmer, J., Hong-Hermesdorf, A., Stierhof, Y. and Schumacher, K. (2006) Vacuolar H^+-ATPase activity is required for endocytic and secretory trafficking in Arabidopsis. *Plant Cell* 18: 715–730.

Drakakaki, G., van de Ven, W., Pan, S., Miao, Y., Wang, J., Keinath, N.F. et al. (2012) Isolation and proteomic analysis of the SYP61 compartment reveal its role in exocytic trafficking in Arabidopsis. *Cell Res.* 22: 413–424.

Driouich, A., Zhang, G.F. and Staehelin, L.A. (1993) Effect of brefeldin A on the structure of the Golgi apparatus and on the synthesis

and secretion of proteins and polysaccharides in sycamore maple (*Acer pseudoplatanus*) suspension-cultured cells. *Plant Physiol.* 101: 1363–1373.

Gendre, D., Oh, J., Boutté, Y., Best, J.G., Samuels, L., Nilsson, R. et al. (2011) Conserved Arabidopsis ECHIDNA protein mediates *trans*-Golgi-network trafficking and cell elongation. *Proc. Natl Acad. Sci. USA* 108: 8048–8053.

Gendre, D., McFarlane, H.E., Johnson, E., Mouille, G., Sjödin, A., Oh, J. et al. (2013) Trans-Golgi network localized ECHIDNA/Ypt interacting protein complex is required for the secretion of cell wall polysaccharides in Arabidopsis. *Plant Cell* 25: 2633–2646.

Haughn, G.W. and Somerville, C. (1986) Sulfonylurea-resistant mutants of Arabidopsis thaliana. *Mol. Gen. Genet.* 204: 430–434.

Hayashi, Y., Yamada, K., Shimada, T., Matsushima, R., Nishizawa, N., Nishimura, M. et al. (2001) A proteinase-storing body that prepares for cell death or stresses in the epidermal cells of Arabidopsis. *Plant Cell Physiol.* 42: 894–899.

Herman, E.M. (2008) Endoplasmic reticulum bodies: solving the insoluble. *Curr. Opin. Plant Biol.* 11: 672–679.

Huss, M., Ingenhorst, G., Konig, S., Gassel, M., Drose, S., Zeeck, A. et al. (2002) Concanamycin A, the specific inhibitor of V-ATPases, binds to the V(o) subunit c. *J. Biol. Chem.* 277: 40544–40548.

Inadome, H., Noda, Y., Kamimura, Y., Adachi, H. and Yoda, K. (2007) Tvp38, Tvp23, Tvp18 and Tvp15: novel membrane proteins in the Tlg2-containing Golgi/endosome compartments of *Saccharomyces cerevisiae*. *Exp. Cell Res.* 313: 688–697.

Jauh, G., Phillips, T.E. and Rogers, J.C. (1999) Tonoplast intrinsic protein isoforms as markers for vacuolar functions. *Plant Cell* 11: 1867–1882.

Leucci, M., Di Sansebastiano, G., Gigante, M., Dalessandro, G. and Piro, G. (2007) Secretion marker proteins and cell-wall polysaccharides move through different secretory pathways. *Planta* 225: 1001–1017.

McFarlane, H.E., Young, R.E., Wasteneys, G.O. and Samuels, A.L. (2008) Cortical microtubules mark the mucilage secretion domain of the plasma membrane in Arabidopsis seed coat cells. *Planta* 227: 1363–1375.

Pattathil, S., Avci, U., Baldwin, D., Swennes, A.G., McGill, J.A., Popper, Z. et al. (2010) A comprehensive toolkit of plant cell wall glycan-directed monoclonal antibodies. *Plant Physiol.* 153: 514–525.

Robert, S., Chary, S.N., Drakakaki, G., Li, S., Yang, Z., Raikhel, N.V. et al. (2008) Endosidin1 defines a compartment involved in endocytosis of the brassinosteroid receptor BRI1 and the auxin transporters PIN2 and AUX1. *Proc. Natl Acad. Sci. USA* 105: 8464–8469.

Robinson, D.G., Albrecht, S. and Moriysu, Y. (2004) The V-ATPase inhibitors concanamycin A and bafilomycin A lead to Golgi swelling in tobacco BY-2 cells. *Protoplasma* 224: 255–260.

Sandhu, A.P.S., Randhawa, G.S. and Dhugga, K.S. (2009) Plant cell wall matrix polysaccharide biosynthesis. *Mol. Plant* 2: 840–850.

Stein, I.S., Gottfried, A., Zimmermann, J. and Fischer von Mollard, G. (2009) TVP23 interacts genetically with the yeast SNARE VTI1 and functions in retrograde transport from the early endosome to the late Golgi. *Biochem. J.* 419: 229–236.

Takatsuka, C., Inoue, Y., Higuchi, T., Hillmer, S., Robinson, D.G. and Moriyasu, Y. (2011) Autophagy in tobacco BY-2 cells cultured under sucrose starvation conditions: isolation of the autolysosome and its characterization. *Plant Cell Physiol.* 52: 2074–2087.

Toyooka, K., Goto, Y., Asatsuma, S., Koizumi, M., Mitsui, T. and Matsuoka, K. (2009) A mobile secretory vesicle cluster involved in mass transport from the Golgi to the plant cell exterior. *Plant Cell* 21: 1212–1229.

Western, T.L., Skinner, D.J. and Haughn, G.W. (2000) Differentiation of mucilage secretory cells of the Arabidopsis seed coat. *Plant Physiol.* 122: 345–356.

Worden, N., Park, E. and Drakakaki, G. (2012) Trans-Golgi network—an intersection of trafficking cell wall components. *J. Integr. Plant Biol.* 54: 875–886.

Young, R.E., McFarlane, H.E., Hahn, M.G., Western, T.L., Haughn, G.W. and Samuels, A.L. (2008) Analysis of the golgi apparatus in arabidopsis seed coat cells during polarized secretion of pectin-rich mucilage. *Plant Cell* 20: 1623–1638.

Zhang, G.F., Driouich, A. and Staehelin, L.A. (1993) Effect of monensin on plant Golgi: re-examination of the monensin-induced changes in cisternal architecture and functional activities of the Golgi apparatus of sycamore suspension-cultured cells. *J. Cell Sci.* 104: 819–831.

Zhang, G.F., Driouich, A. and Staehelin, L.A. (1996) Monensin-induced redistribution of enzymes and products from Golgi stacks to swollen vesicles. *Eur. J. Cell Biol.* 71: 332–340.

Zheng, H., Kunst, L., Hawes, C. and Moore, I. (2004) A GFP-based assay reveals a role for RHD3 in transport between the endoplasmic reticulum and Golgi apparatus. *Plant J.* 37: 398–414.